Original Article

A correlative study between IVIM-DWI parameters and VEGF and MMPs expression in hepatocellular carcinoma

Cui Yang[1,2#^], Xiao-Qin Wei[3#^], Jing Zheng[1^], Yun-Yun Tao[1^], Xue-Qin Gong[1^], Li Li[4], Zu-Mao Li[4^], Lin Yang[1^], Qi Mao[1^], Mao-Ting Zhou[1^], Xiao-Ming Zhang[1^]

[1]Medical Imaging Key Laboratory of Sichuan Province, Department of Radiology and Medical Research Center, Affiliated Hospital of North Sichuan Medical College, Nanchong, China; [2]Department of Radiology, Panzhihua Central Hospital, Panzhihua, China; [3]School of Medical Imaging of North Sichuan Medical College, Nanchong, China; [4]Department of Pathology, Affiliated Hospital of North Sichuan Medical College, Nanchong, China

Contributions: (I) Conception and design: L Yang, XM Zhang; (II) Administrative support: XM Zhang; (III) Provision of study materials or patients: L Li, ZM Li, L Yang; (IV) Collection and assembly of data: C Yang, J Zheng, YY Tao, XQ Gong, Q Mao, MT Zhou; (V) Data analysis and interpretation: C Yang, XQ Wei, ZM Li, L Yang; (VI) Manuscript writing: All authors; (VII) Final approval of manuscript: All authors.

[#]These authors contributed equally to this work.

Correspondence to: Lin Yang. Medical Imaging Key Laboratory of Sichuan Province, Department of Radiology and Medical Research Center, Affiliated Hospital of North Sichuan Medical College, Nanchong 637000, China. Email: linyangmd@163.com.

Background: Hepatocellular carcinoma (HCC) is the fourth most common cause of cancer-related death worldwide. Angiogenic factors may be valuable indices of tumor recurrence and treatment and potentially useful markers for predicting the response to antiangiogenesis therapy. Vascular endothelial growth factor (VEGF) and matrix metalloproteinases (MMPs) are major drivers of tumor angiogenesis. Preoperatively predicting the expression of VEGF and MMPs is crucial for treating HCC. Intravoxel incoherent motion (IVIM) diffusion-weighted imaging (DWI) has been successfully used in the differential diagnosis of HCC, pathological grading, and treatment response evaluation. However, the correlations between IVIM-DWI parameters and VEGF and MMP expression have not been reported. This study provides a preliminary analysis of the correlation between IVIM-DWI parameters and the expression of VEGF, MMP-2, and MMP-9 to investigate the value of IVIM-DWI in the noninvasive evaluation of angiogenesis in HCC.

Methods: IVIM-DWI was performed in 61 patients with HCC 1 week before they underwent surgical resection. VEGF, MMP-2, and MMP-9 expression was detected using immunohistochemistry staining. Spearman correlation analysis was used to analyze the correlations between the IVIM-DWI parameters and VEGF, MMP-2, and MMP-9 expression in HCC.

Results: The fast apparent diffusion coefficient fraction (*f*) value was positively correlated with the expression of VEGF (P<0.001), MMP-2 (P=0.002), and MMP-9 (P<0.001). The fast apparent diffusion coefficient (*D**) was positively correlated with VEGF (P<0.001) and MMP-9 (P<0.001) expression but was not correlated with MMP-2 (P=0.659) expression. The apparent diffusion coefficient (ADC) and slow apparent diffusion coefficient (*D*) values were not significantly correlated with the expression of VEGF (P=0.103 and P=0.543, respectively), MMP-2 (P=0.596 and P=0.338, respectively), or MMP-9 (P=0.102 and P=0.660, respectively).

Conclusions: IVIM-DWI can be used to noninvasively evaluate angiogenesis in HCC.

^ ORCID: Cui Yang, 0000-0001-6751-9075; Xiao-Qin Wei, 0000-0001-5341-9970; Jing Zheng, 0000-0002-2031-0845; Yun-Yun Tao, 0000-0001-5081-3315; Xue-Qin Gong, 0000-0001-8389-8765; Zu-Mao Li, 0000-0002-1495-0977; Lin Yang, 0000-0001-8746-9255; Qi Mao, 0000-0003-1301-069X; Mao-Ting Zhou, 0000-0003-2034-2086; Xiao-Ming Zhang, 0000-0001-5327-8506.

Keywords: Hepatocellular carcinoma (HCC); vascular endothelial growth factor (VEGF); matrix metalloproteinase (MMP); angiogenesis; intravoxel incoherent motion (IVIM); diffusion-weighted imaging (DWI)

Submitted Mar 24, 2022. Accepted for publication Nov 10, 2022. Published online Jan 02, 2023.
doi: 10.21037/qims-22-271
View this article at: https://dx.doi.org/10.21037/qims-22-271

Introduction

Hepatocellular carcinoma (HCC) is the fourth most common cause of cancer-related death in the world (1,2). Tumor growth can be limited by suppressing tumor angiogenesis. Angiogenic factors have been identified as valuable indices of recurrence in the treatment of tumors and as useful markers to predict antiangiogenesis therapy response (3). Among these factors, vascular endothelial growth factor (VEGF) and matrix metalloproteinases (MMPs) are major drivers of tumor angiogenesis. Preoperatively predicting VEGF and MMP expression is critical to treating HCC.

Intravoxel incoherent motion diffusion-weighted imaging (IVIM-DWI) is a new technology that has emerged in recent years. Using a biexponential model, IVIM-DWI can quantitatively measure information related to pure water molecule diffusion and microcirculation perfusion, thus compensating for the shortcomings of traditional DWI. Recently, IVIM-DWI has been successfully used in differential diagnosis (4), pathological grading (5-7), assessment of microvascular invasion (MVI) (7), and evaluation of treatment response (8). Several studies have investigated the relationship between apparent diffusion coefficients (ADCs) derived from traditional DWI and VEGF expression in various tumors, but the reported results are contradictory (9-11).

However, there are no reports on the use of IVIM-DWI to evaluate the expression of VEGF and MMPs in HCC. This study provides a preliminary analysis of the correlation between IVIM-DWI parameters and the expression of VEGF, MMP-2, and MMP-9 to investigate the value of IVIM-DWI in the noninvasive evaluation of angiogenesis in HCC.

Methods

Patient data

The study was conducted in accordance with the Declaration of Helsinki (as revised in 2013). This study was approved by the Ethics Committee of the Affiliated Hospital of North Sichuan Medical College. Written informed consent was obtained from all study participants. A total of 393 patients with HCC who visited the Affiliated Hospital of North Sichuan Medical College between January 2018 and September 2019 were included. The final cohort consisted of 61 patients with HCC who had no other liver diseases according to the inclusion and exclusion criteria (*Figure 1*). Patients were included if they (I) had received surgery within 1 week after magnetic resonance imaging (MRI) examination, (II) had not received preoperative radiochemotherapy or preoperative interventional therapy, and (III) had a postoperative pathological diagnosis of HCC. Patients were excluded if they (I) had contraindications for MRI examination or (II) had incomplete data or poor image quality.

MRI scan and data measurement

All patients underwent conventional noncontrast-enhanced MRI, dynamic contrast-enhanced MRI, and IVIM-DWI imaging using a 3.0T magnetic resonance scanner with a 32-channel phased array body coil (Discovery MR750, GE Healthcare, Chicago, IL, USA). Patients had fasted for more than 4 hours and completed respiration training before the MRI scans. Each patient was scanned from the apex of the diaphragm to the lower edge of the liver. The MRI sequence and parameters and the data measurement method used in this study were the same as those used in previous studies (12,13). The IVIM-DWI sequence (respiratory-triggered) was obtained using the following parameters: repetition time/time to echo (TR/TE), 3529/60.8 ms; flip angle (FA), 90°; matrix, 128×160; field of view (FOV), 340×340 mm^2 to 360×360 mm^2; and section thickness, 5 mm. Nine *b* values (*b*=0, 20, 50, 100, 150, 200, 400, 800, and 1,000 s/mm^2) were used for the IVIM-DWI sequence, and segmented fitting with a threshold *b* value of 200 s/mm^2 was used. The contrast-enhanced MRI sequence was acquired after IVIM-DWI. The contrast agent (Gd-DTPA; 15–20 mL) was injected with a high-pressure

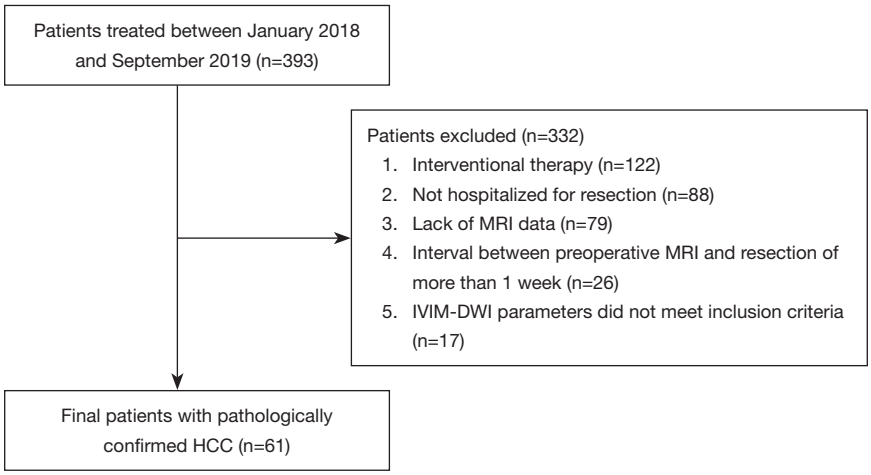

Figure 1 Flowchart of the study population. HCC, hepatocellular carcinoma; IVIM-DWI, intravoxel incoherent motion diffusion-weighted imaging; MRI, magnetic resonance imaging.

syringe through the vein of the hand at an injection speed of 2–2.5 mL/s.

MR images were sent to a GE ADW4.6 workstation and analyzed using Function-MADC software. A 70–80 mm^2 region of interest (ROI) was manually selected in the largest solid area of the HCC lesion, with areas with necrosis, hemorrhage, or cystic degeneration being avoided. Pseudocolor parameter maps of the ADC, slow apparent diffusion coefficient (*D*), fast apparent diffusion coefficient (*D**), and fast apparent diffusion coefficient fraction (*f*) were generated. All parameter values were measured 3 times, and the average values were recorded.

Immunohistochemical staining

The VEGF, MMP-9, and MMP-2 antibodies (Abcam, Cambridge, UK) were clones ab1316, ab38898, and ab86607, respectively, and their dilutions were 1:200, 1:250, and 1:250, respectively. Postoperative HCC tissue specimens were fixed in 10% formalin, dehydrated in ethanol, cleared in xylene, embedded in paraffin, and serially sectioned into 5-μm slices for hematoxylin and eosin (HE) staining and immunohistochemical staining. The VEGF, MMP-9, and MMP-2 staining results were evaluated based on the semiquantitative method of Shimizu *et al.* (14,15).

Scores for the proportion of stained cells were as follows: 0 points indicated that no cells were stained, 1 point indicated that 1–10% of tumor cells stained positively, 2 points indicated that 11–50% of tumor cells stained positively, and 3 points indicated that 51–100% of tumor cells stained positively.

Scores for staining intensity were as follows: 0 points indicated that no cells were stained, 1 point indicated that the tumor cells stained light yellow, 2 points indicated that the tumor cells stained brownish yellow, and 3 points indicated that the tumor cells stained brown.

The overall score was defined as the sum of the scores for the proportion of stained cells and for staining intensity: overall score = score for the proportion of stained cells + score for staining intensity. The overall score was divided into 3 levels: 0–2 points represented negative, 3–4 points represented positive, and 5–6 points represented strongly positive.

Statistical analysis

All data were statistically analyzed using SPSS 23.0 (IBM Corp, Armonk, NY, USA). One-way analysis of variance was used to compare the differences in IVIM-DWI parameters between HCC tissues with negative, positive, and strongly positive expressions of VEGF, MMP-9, and MMP-2.

Spearman correlation analysis was used to analyze the correlation between the IVIM-DWI parameters and the expression of VEGF, MMP-9, and MMP-2 in HCC tissues. A P value less than 0.05 indicated a statistically significant difference.

Results

The 61 patients in this study included 55 males and 6 females aged 29 to 70 years; the average age was 50.3±10.4 years. The tumor size ranged from 1.2 to 16.1 cm with an average size of 5.1±3.3 cm. VEGF expression was negative in 10 patients, positive in 39 patients, and strongly positive in 12 patients. MMP-9 expression was negative in 12 patients, positive in 30 patients, and strongly positive in 19 patients. MMP-2 expression was negative in 17 patients, positive in 36 patients, and strongly positive in 8 patients.

The *f* value was significantly different among patients with different expression levels of VEGF, MMP-2, and MMP-9. The *f* values of patients strongly positive for VEGF, MMP-2, and MMP-9 were significantly higher than those of patients who were positive or negative for VEGF, MMP-2, and MMP-9. The *f* values of patients positive for VEGF, MMP-2, and MMP-9 were significantly greater than those of patients negative for VEGF, MMP-2, and MMP-9, respectively. The *D** value was significantly different between patients with different expression levels of VEGF and MMP-9 and was not significantly different between patients with different expression levels of MMP-2. The *D** values of patients who were strongly positive for VEGF and MMP-9 were greater than those of patients positive for VEGF or negative for MMP-9. The *D** values of patients positive for VEGF and MMP-9 were greater than those of patients negative for VEGF and MMP-9. The ADC and *D* value were not significantly different among patients with different expression levels of VEGF, MMP-2, and MMP-9.

The *f* value was positively correlated with the expression of VEGF, MMP-2, and MMP-9. The *D** value was positively correlated with VEGF and MMP-9 expression but was not correlated with MMP-2 expression. ADC and *D* values did not significantly correlate with the expression of VEGF, MMP-2, or MMP-9 (*Tables 1*,*2*; *Figures 2-4*).

Discussion

Le Bihan (16) was first to propose the concept of IVIM in the 1980s. IVIM-DWI refers to diffusion-weighted imaging based on a double exponential model that can quantitatively obtain information on water molecule diffusion and microcirculatory perfusion-related diffusion. It compensates for a deficiency of the conventional single exponential model–based DWI, which can only determine the ADC (17). *D*, an IVIM-DWI parameter, reflects the diffusion of water molecules in the tissue within the ROI; *D** reflects the microcirculatory perfusion in the ROI; *f* represents the ratio of microcirculatory perfusion-related diffusion volume to total diffusion volume (18-20). The attenuation of the IVIM-DWI signal in tissue is related to the *b* value (18,21):

$$S_b / S_0 = (1-f)\times\exp(-bD) + f\times\exp\left[-b(D+D^*)\right] \quad [1]$$

where S_b and S_0 are the signal intensities at *b* values of *b* and 0 s/mm^2, respectively (21).

VEGF is an endothelial cell–specific mitogen that induces angiogenesis (22). VEGF plays an important role in mediating tumor angiogenesis (23-28). MMPs are zinc-dependent endopeptidases with proteolytic enzyme activity that play an important role in extracellular matrix remodeling and affect tumor growth, invasion, and distant metastasis (29,30). MMP-2 and MMP-9 are important members of the MMP family and are the 2 most effective initiators of collagen breakdown (30). They play a key role in the angiogenesis, invasion, and metastasis of HCC (31,32). In tumor angiogenesis, there is a complex mutual regulatory relationship between VEGF and MMPs (33-36).

Microvessel density (MVD) is commonly used to evaluate tissue perfusion. Perfusion-related IVIM-DWI parameters, such as *D** and *f*, and the expression of angiogenic factors, such as VEGF, MMP-2, and MMP-9, in tumor tissue are significantly positively correlated with MVD (31,32,37-41). IVIM-DWI parameters can be used to evaluate tumor angiogenesis (40,42,43). An IVIM-DWI study of a mouse lung cancer model showed that *D** and *f* were positively correlated with VEGF expression (43). A study using MR-DWI to monitor how metastatic abdominal and pelvic tumors responded to a VEGF inhibitor showed that *D** significantly decreased on day 7 and that *f* significantly decreased on day 28 (44). Significant differences in the *f* values of colorectal cancer patients with different expression levels of mismatch repair proteins may be related to the differential expression of VEGF and its receptor, VEGFR2 (40). However, *D** is reported to have no correlation with VEGF (42). The possible causes of these controversial findings may be that the structure and density of some capillaries cannot reflect the information from macroscopic tumors and blood vessels (42); other physiological processes, such as glandular secretion and fluid flows inside the glandular ducts and other ducts, may affect the measured *D** values (45), and *D** is associated with a low signal-to-noise ratio (46) and poor

Table 1 Comparison of IVIM-DWI parameters for patients with different expression levels of VEGF, MMP-2, and MMP-9 in HCC tissues

Biomarker	ADC (10^{-3} mm^2/s)	D (10^{-3} mm^2/s)	D^* (10^{-3} mm^2/s)	f (%)
VEGF				
Negative	1.04±0.17	0.84±0.20	26.03±19.84[a]	13.51±5.03[a]
Positive	1.20±0.25	0.89±0.19	44.51±21.31[b]	22.41±6.76[b]
Strongly positive	1.21±0.17	0.95±0.18	66.01±18.49[c]	33.78±5.48[c]
F	2.236	0.994	10.483	29.132
P value	0.116	0.376	0.000	0.000
MMP-2				
Negative	1.17±0.21	0.92±0.14	47.09±26.83	18.67±8.68[a]
Positive	1.17±0.24	0.88±0.22	42.16±21.49	23.37±7.18[b]
Strongly positive	1.21±0.24	0.91±0.10	58.77±23.58	31.99±9.44[c]
F	0.099	0.238	1.700	0.717
P value	0.906	0.789	0.192	0.001
MMP-9				
Negative	1.06±0.23	0.88±0.19	27.76±15.34[a]	14.56±4.64[a]
Positive	1.20±0.23	0.89±0.21	42.81±22.34[b]	22.28±6.92[b]
Strongly positive	1.20±0.21	0.92±0.17	61.63±20.32[c]	30.08±8.02[c]
F	2.006	0.215	10.578	18.969
P value	0.144	0.807	0.000	0.000

The values of ADC, D, D^*, and f are presented as mean ± standard deviation. Superscript letters indicate significant differences between groups. D, slow apparent diffusion coefficient; D^*, fast apparent diffusion coefficient; f, fast apparent diffusion coefficient fraction. HCC, hepatocellular carcinoma; VEGF, vascular endothelial growth factor; MMP, matrix metalloproteinase; IVIM-DWI, intravoxel incoherent motion diffusion-weighted imaging; ADC, apparent diffusion coefficient.

Table 2 Correlation between IVIM-DWI parameters and the expression of VEGF, MMP-2, and MMP-9 in HCC tissues

Parameters	VEGF		MMP-2		MMP-9	
	r	P value	r	P value	r	P value
ADC	0.211	0.103	–0.069	0.596	0.212	0.102
D	0.079	0.543	–0.125	0.338	0.057	0.660
D^*	0.526	0.000	0.058	0.659	0.488	0.000
f	0.740	0.000	0.387	0.002	0.633	0.000

D, slow apparent diffusion coefficient; D^*, fast apparent diffusion coefficient; f, fast apparent diffusion coefficient fraction. HCC, hepatocellular carcinoma; VEGF, vascular endothelial growth factor; MMP, matrix metalloproteinases; IVIM-DWI, intravoxel incoherent motion diffusion-weighted imaging; ADC, apparent diffusion coefficient.

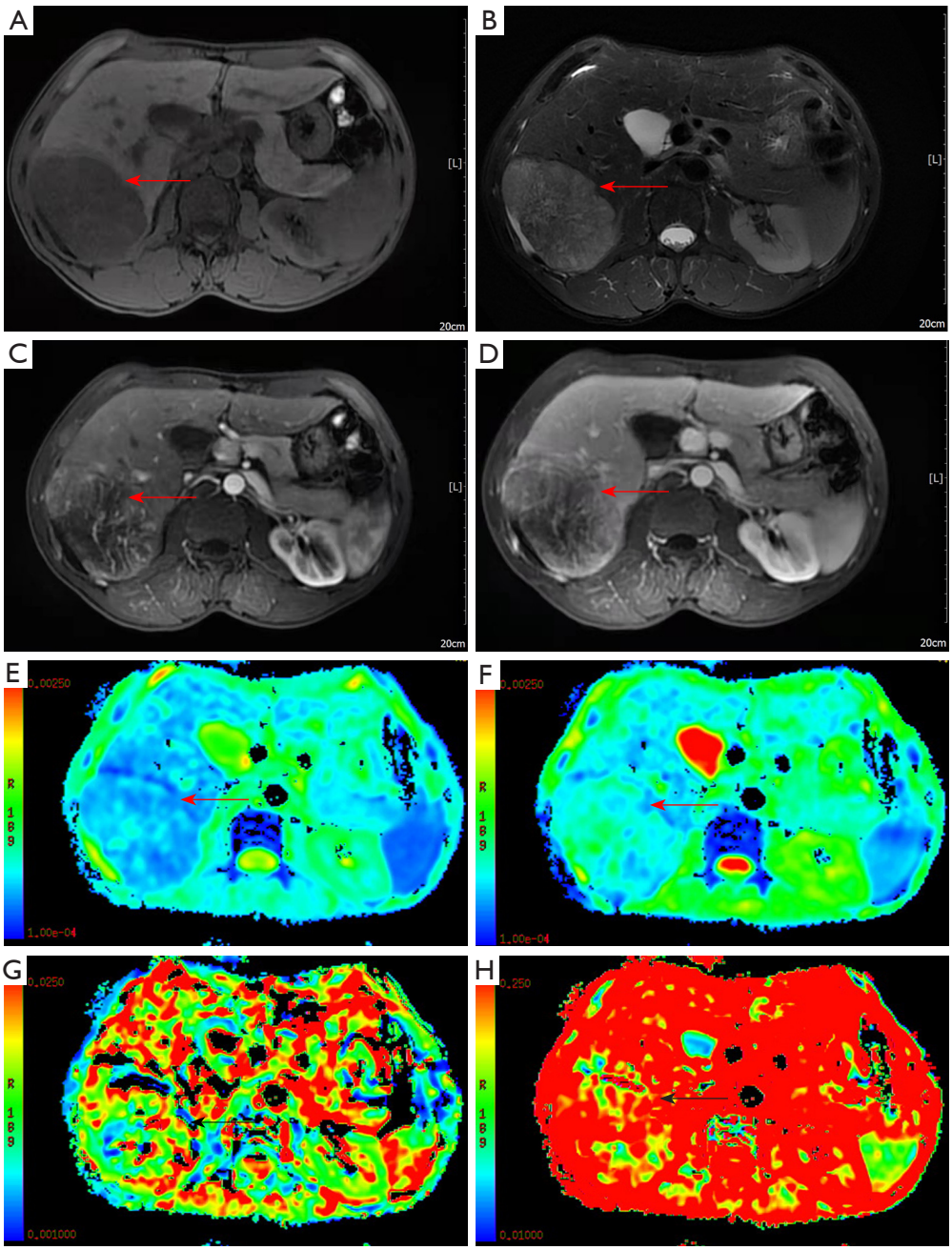

Figure 2 Images of a 33-year-old male with HCC in the right lobe of the liver. (A) Unenhanced T1-weighted image showing a mildly hypointense lesion (red arrow). (B) Unenhanced T2-weighted image showing a heterogeneous and mildly hyperintense lesion (red arrow). (C) An image of the arterial phase showing a significantly unevenly enhanced lesion (red arrow). (D) An image of the portal venous phase showing a lesion with reduced enhancement (red arrow). (E) The map of the ADC (red arrow) showing an ADC of 1.29×10^{-3} mm^2/s. (F) The map of the *D* (red arrow) showing a *D* value of 0.93×10^{-3} mm^2/s. (G) Map of the *D** (black arrow) showing a *D** value of 33.8×10^{-3} mm^2/s. (H) The map of the *f* (black arrow) showing an *f* value of 19.5%. HCC, hepatocellular carcinoma; ADC, apparent diffusion coefficient; *D*, slow apparent diffusion coefficient; *D**, fast apparent diffusion coefficient; *f*, fast apparent diffusion coefficient fraction.

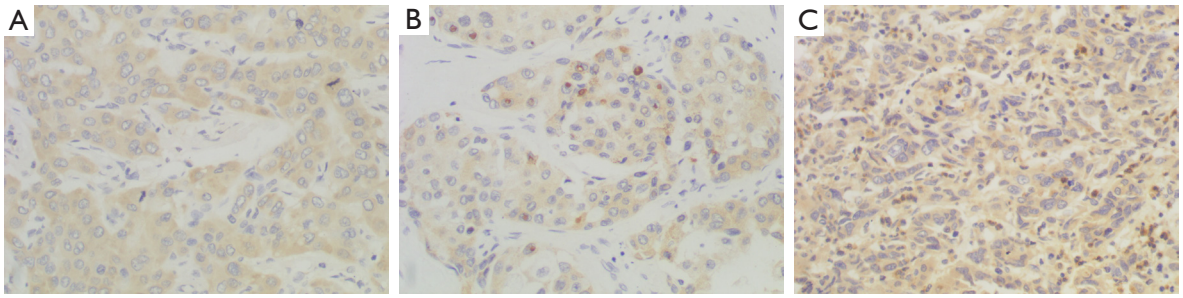

Figure 3 Immunohistochemistry images of VEGF, MMP-2, and MMP-9, all showing strong positivity. (A) VEGF (×200); (B) MMP-2 (×200); (C) MMP-9 (×200). VEGF, vascular endothelial growth factor; MMP, matrix metalloproteinase.

stability (18,47). In this study, *D** was positively correlated with the expression of VEGF and MMP-9, and *f* was positively correlated with the expression of VEGF, MMP-9, and MMP-2, suggesting that perfusion-related IVIM-DWI parameters could reflect angiogenesis in HCC.

The correlations between the IVIM-DWI parameters ADC and *D* and tumor angiogenesis are inconsistent across different studies (10,39,40,44,48-51). Li *et al.* (51) showed a statistically significant correlation between the *D* value and MVD. In contrast, Lee *et al.* (39) found no significant correlation between tissue diffusivity (*Dt*) and MVD. Regarding the relationships between the IVIM-DWI parameters ADC and *D* and the angiogenic factors VEGF and MMPs, some studies have shown that ADC is negatively correlated with VEGF (10,49-50), MMP-9, and MMP-2 (15) expression, while other studies have shown that ADC is positively correlated (52) or nonsignificantly (11,53,54) correlated with VEGF expression. These inconsistent results might be related to a number of factors. First, the relationship between VEGF and MMP expression and tumor angiogenesis is complex (55). Second, VEGF expression leads to the proliferation of tumor cells and restricted movement of intracellular and extracellular water molecules, which can decrease ADC values (10). On the other hand, it leads to more tumor blood vessels, faster proton movement in lumens, and increased ADC values (52). Third, VEGF expression is already high in the early stage of tumor development and does not increase exponentially with tumor growth (52). Fourth, in addition to VEGF and MMPs, other angiogenic factors are also involved in tumor angiogenesis (55,56). Fifth, factors such as sample size, *b* value, and distribution may also affect the measured results (16,18,57).

The results of this study indicated no significant correlations between the IVIM-DWI parameters ADC and *D* and the angiogenic factors VEGF, MMP-2, and MMP-9. Further research is needed in the future.

This study has some limitations. First, the relationship between the IVIM-DWI parameters and the degree of HCC tissue enhancement was not investigated. Second, due to tumor heterogeneity, the values of the IVIM-DWI parameters obtained from selective ROIs could not fully represent the overall tumor condition. Third, the number and size distributions of *b* values are not yet standardized and thus require further optimization (58,59). In addition, according to current IVIM models, the mutual constraint of the diffusion and perfusion components occurs (changing toward the opposite direction) (60-62). Recently, Wáng *et al.* (60-62) reported that liver microperfusion could be evaluated by diffusion-derived vessel density (DDVD). The *D**, *f*, and DDVD values measure different aspects of liver perfusion. The *D** and *f* values may mainly measure the arteries, while DDVD may mainly measure the veins rather than the arteries. Moreover, the DDVD is not constrained by IVIM-DWI modeling. In the future, conventional IVIM-DWI parameters integrating the DDVD may improve the diagnostic performance of liver DWI (60-62).

Conclusions

In conclusion, the results of the present study suggest that IVIM-DWI can be used to noninvasively evaluate angiogenesis in HCC.

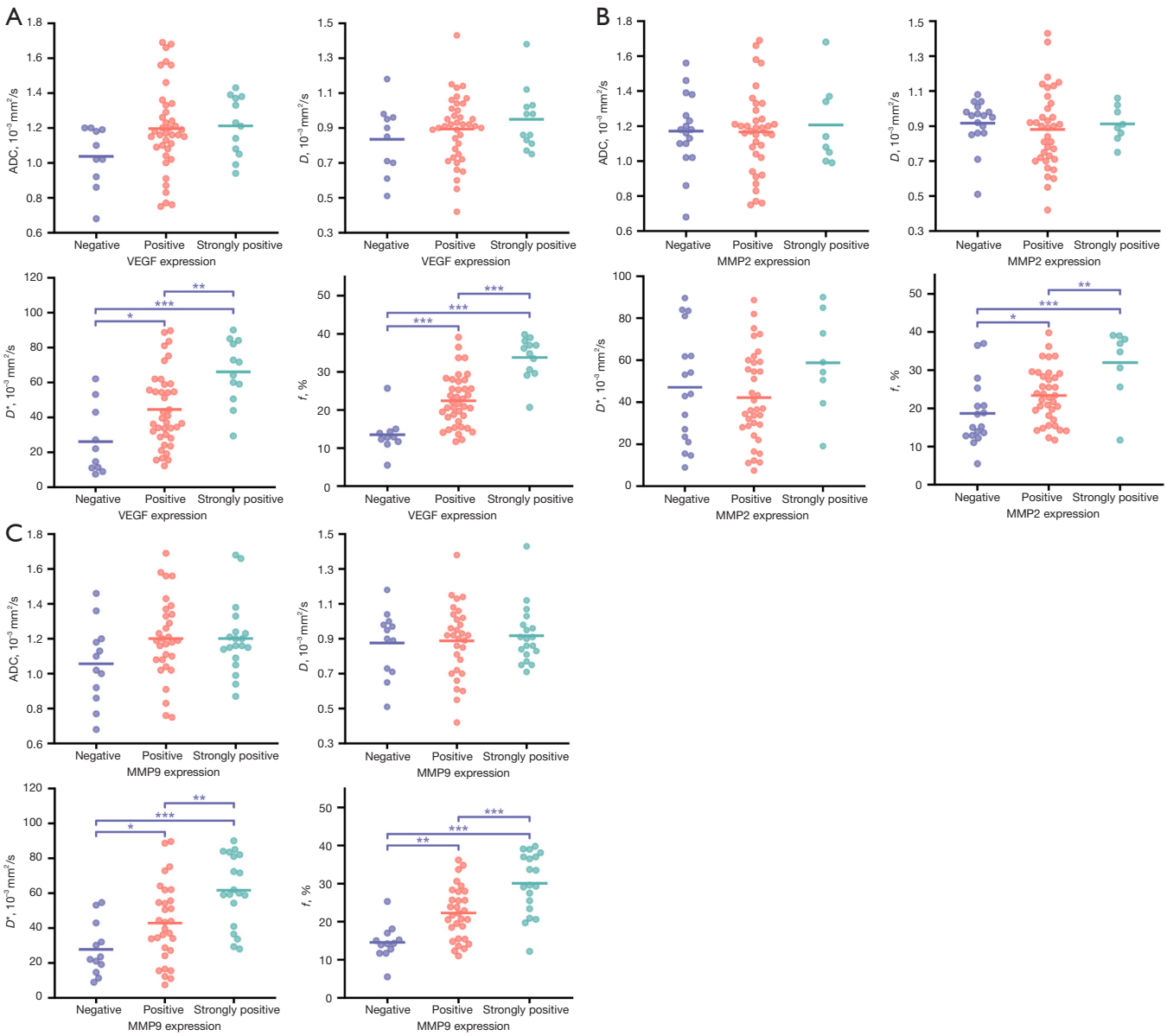

Figure 4 Scatter plots showing the correlation between IVIM-DWI parameters and VEGF (A), MMP-2 (B), and MMP-9 (C) expression in HCC. The ADC, D, and *D** value unit is $\times 10^{-3}$ mm^2/s, and the *f* value unit is %. *, indicates P<0.05; **, indicates P<0.01; ***, indicates P<0.001. *D*, slow apparent diffusion coefficient; *D**, fast apparent diffusion coefficient; *f*, fast apparent diffusion coefficient fraction. IVIM-DWI, intravoxel incoherent motion diffusion-weighted imaging; VEGF, vascular endothelial growth factor; MMP, matrix metalloproteinase; HCC, hepatocellular carcinoma; ADC, apparent diffusion coefficient.

Acknowledgments

Funding: This work was supported by the Department of Science and Technology of Sichuan Province (No. 2016JY0105), the Medical Association of Sichuan Province (No. S20070), and the City-University Science and Technology Strategic Cooperation of Nanchong City (No. 20SXQT0324).

Footnote

Conflicts of Interest: All authors have completed the ICMJE uniform disclosure form (available at https://qims.

amegroups.com/article/view/10.21037/qims-22-271/coif). The authors have no conflicts of interest to declare.

Ethical Statement: The authors are accountable for all aspects of the work in ensuring that questions related to the accuracy or integrity of any part of the work are appropriately investigated and resolved. The study was conducted in accordance with the Declaration of Helsinki (as revised in 2013). This study was approved by the Ethics Committee of Affiliated Hospital of North Sichuan Medical College. Written informed consent was obtained from all study participants.

References

1. Ozakyol A. Global Epidemiology of Hepatocellular Carcinoma (HCC Epidemiology). J Gastrointest Cancer 2017;48:238-40.
2. Yang JD, Hainaut P, Gores GJ, Amadou A, Plymoth A, Roberts LR. A global view of hepatocellular carcinoma: trends, risk, prevention and management. Nat Rev Gastroenterol Hepatol 2019;16:589-604.
3. Goel S, Duda DG, Xu L, Munn LL, Boucher Y, Fukumura D, Jain RK. Normalization of the vasculature for treatment of cancer and other diseases. Physiol Rev 2011;91:1071-121.
4. Wu H, Liang Y, Jiang X, Wei X, Liu Y, Liu W, Guo Y, Tang W. Meta-analysis of intravoxel incoherent motion magnetic resonance imaging in differentiating focal lesions of the liver. Medicine (Baltimore) 2018;97:e12071.
5. Granata V, Fusco R, Filice S, Catalano O, Piccirillo M, Palaia R, Izzo F, Petrillo A. The current role and future prospectives of functional parameters by diffusion weighted imaging in the assessment of histologic grade of HCC. Infect Agent Cancer 2018;13:23.
6. Wei Y, Gao FF, Huang ZX, Tang HH, Wang M, Wang Y, Zhang T, Song B. Preliminary study of whole-tumor volume analysis of mono-exponential and intravoxel incoherent motion models in the preoperative histologic grading of hepatocellular carcinoma. Zhonghua Yi Xue Za Zhi 2018;98:2460-5.
7. Surov A, Pech M, Omari J, Fischbach F, Damm R, Fischbach K, Powerski M, Relja B, Wienke A. Diffusion-Weighted Imaging Reflects Tumor Grading and Microvascular Invasion in Hepatocellular Carcinoma. Liver Cancer 2021;10:10-24.
8. Wei Y, Gao F, Zheng D, Huang Z, Wang M, Hu F, Chen C, Duan T, Chen J, Cao L, Song B. Intrahepatic cholangiocarcinoma in the setting of HBV-related cirrhosis: Differentiation with hepatocellular carcinoma by using Intravoxel incoherent motion diffusion-weighted MR imaging. Oncotarget 2017;9:7975-83.
9. Meyer HJ, Wienke A, Surov A. Association Between VEGF Expression and Diffusion Weighted Imaging in Several Tumors-A Systematic Review and Meta-Analysis. Diagnostics (Basel) 2019;9:126.
10. Cong Q, Li G, Wang Y, Zhang S, Zhang H. DW-MRI for esophageal squamous cell carcinoma, correlations between ADC values with histologic differentiation and VEGF expression: A retrospective study. Oncol Lett 2019;17:2770-6.
11. Heo SH, Jeong YY, Shin SS, Kim JW, Lim HS, Lee JH, Koh YS, Cho CK, Kang HK. Apparent diffusion coefficient value of diffusion-weighted imaging for hepatocellular carcinoma: correlation with the histologic differentiation and the expression of vascular endothelial growth factor. Korean J Radiol 2010;11:295-303.
12. Peng J, Zheng J, Yang C, Wang R, Zhou Y, Tao YY, Gong XQ, Wang WC, Zhang XM, Yang L. Intravoxel incoherent motion diffusion-weighted imaging to differentiate hepatocellular carcinoma from intrahepatic cholangiocarcinoma. Sci Rep 2020;10:7717.
13. Zheng J, Gong XQ, Tao YY, Wang R, Yang G, Li JD, Ren T, Li ZM, Yang C, Wang WC, Yang L, Zhang XM. A Correlative Study Between IVIM-DWI Parameters and the Expression Levels of Ang-2 and TKT in Hepatocellular Carcinoma. Front Oncol 2021;10:594366.
14. Shimizu M, Saitoh Y, Itoh H. Immunohistochemical staining of Ha-ras oncogene product in normal, benign, and malignant human pancreatic tissues. Hum Pathol 1990;21:607-12.
15. Xu T, Zhang L, Xu H, Kang S, Xu Y, Luo X, Hua T, Tang G. Prediction of low-risk breast cancer using quantitative DCE-MRI and its pathological basis. Oncotarget 2017;8:114360-70.
16. Le Bihan D, Breton E, Lallemand D, Grenier P, Cabanis

E, Laval-Jeantet M. MR imaging of intravoxel incoherent motions: application to diffusion and perfusion in neurologic disorders. Radiology 1986;161:401-7.
17. Zhang Y, Jin N, Deng J, Guo Y, White SB, Yang GY, Omary RA, Larson AC. Intra-voxel incoherent motion MRI in rodent model of diethylnitrosamine-induced liver fibrosis. Magn Reson Imaging 2013;31:1017-21.
18. Li YT, Cercueil JP, Yuan J, Chen W, Loffroy R, Wáng YX. Liver intravoxel incoherent motion (IVIM) magnetic resonance imaging: a comprehensive review of published data on normal values and applications for fibrosis and tumor evaluation. Quant Imaging Med Surg 2017;7:59-78.
19. Lewin M, Fartoux L, Vignaud A, Arrivé L, Menu Y, Rosmorduc O. The diffusion-weighted imaging perfusion fraction f is a potential marker of sorafenib treatment in advanced hepatocellular carcinoma: a pilot study. Eur Radiol 2011;21:281-90.
20. Surov A, Meyer HJ, Höhn AK, Behrmann C, Wienke A, Spielmann RP, Garnov N. Correlations between intravoxel incoherent motion (IVIM) parameters and histological findings in rectal cancer: preliminary results. Oncotarget 2017;8:21974-83.
21. Le Bihan D, Breton E, Lallemand D, Aubin ML, Vignaud J, Laval-Jeantet M. Separation of diffusion and perfusion in intravoxel incoherent motion MR imaging. Radiology 1988;168:497-505.
22. Ferrara N. Vascular endothelial growth factor: basic science and clinical progress. Endocr Rev 2004;25:581-611.
23. Shibuya M. VEGF-VEGFR System as a Target for Suppressing Inflammation and other Diseases. Endocr Metab Immune Disord Drug Targets 2015;15:135-44.
24. Bender RJ, Mac Gabhann F. Dysregulation of the vascular endothelial growth factor and semaphorin ligand-receptor families in prostate cancer metastasis. BMC Syst Biol 2015;9:55.
25. Nicosia RF. What is the role of vascular endothelial growth factor-related molecules in tumor angiogenesis? Am J Pathol 1998;153:11-6.
26. Bry M, Kivelä R, Leppänen VM, Alitalo K. Vascular endothelial growth factor-B in physiology and disease. Physiol Rev 2014;94:779-94.
27. Yang ZF, Poon RT. Vascular changes in hepatocellular carcinoma. Anat Rec (Hoboken) 2008;291:721-34.
28. Tseng PL, Tai MH, Huang CC, Wang CC, Lin JW, Hung CH, Chen CH, Wang JH, Lu SN, Lee CM, Changchien CS, Hu TH. Overexpression of VEGF is associated with positive p53 immunostaining in hepatocellular carcinoma (HCC) and adverse outcome of HCC patients. J Surg Oncol 2008;98:349-57.
29. Fink K, Boraty ski J. The role of metalloproteinases in modification of extracellular matrix in invasive tumor growth, metastasis and angiogenesis. Postepy Hig Med Dosw (Online) 2012;66:609-28.
30. Tang Y, Nakada MT, Kesavan P, McCabe F, Millar H, Rafferty P, Bugelski P, Yan L. Extracellular matrix metalloproteinase inducer stimulates tumor angiogenesis by elevating vascular endothelial cell growth factor and matrix metalloproteinases. Cancer Res 2005;65:3193-9.
31. Zhao WB, Li Y, Liu X, Zhang LY, Wang X. Evaluation of PRL-3 expression, and its correlation with angiogenesis and invasion in hepatocellular carcinoma. Int J Mol Med 2008;22:187-92.
32. Sun MH, Han XC, Jia MK, Jiang WD, Wang M, Zhang H, Han G, Jiang Y. Expressions of inducible nitric oxide synthase and matrix metalloproteinase-9 and their effects on angiogenesis and progression of hepatocellular carcinoma. World J Gastroenterol 2005;11:5931-7.
33. Deryugina EI, Quigley JP. Tumor angiogenesis: MMP-mediated induction of intravasation- and metastasis-sustaining neovasculature. Matrix Biol 2015;44-46:94-112.
34. Ii M, Yamamoto H, Adachi Y, Maruyama Y, Shinomura Y. Role of matrix metalloproteinase-7 (matrilysin) in human cancer invasion, apoptosis, growth, and angiogenesis. Exp Biol Med (Maywood) 2006;231:20-7.
35. Liu K, Min XL, Peng J, Yang K, Yang L, Zhang XM. The Changes of HIF-1α and VEGF Expression After TACE in Patients With Hepatocellular Carcinoma. J Clin Med Res 2016;8:297-302.
36. Liu K, Yang L, Zhang XM, Zhou Y, Zhu T, Miao ND, Ren YJ, Xu H, Min XL, Peng J, Yang K, Yang S. HIF-1α and VEGF levels for monitoring hepatocellular carcinoma treatment response to transcatheter arterial chemoembolization. Transl Cancer Res 2017;6:1043-9.
37. Zhang Q, Chen X, Zhou J, Zhang L, Zhao Q, Chen G, Xu J, Qian F, Chen Z. CD147, MMP-2, MMP-9 and MVD-CD34 are significant predictors of recurrence after liver transplantation in hepatocellular carcinoma patients. Cancer Biol Ther 2006;5:808-14.
38. Guo RP, Zhong C, Shi M, Zhang CQ, Wei W, Zhang YQ, Li JQ. Expression and clinical significance of certain apoptosis and angiogenesis factors in hepatocellular carcinoma. Zhonghua Wai Ke Za Zhi 2006;44:1626-30.
39. Lee HJ, Rha SY, Chung YE, Shim HS, Kim YJ, Hur J, Hong YJ, Choi BW. Tumor perfusion-related parameter of diffusion-weighted magnetic resonance imaging: correlation with histological microvessel density. Magn

Reson Med 2014;71:1554-8.
40. Yan C, Liu S, Pan X, Chen G, Ge W, Guan W, Liu S, Li M, He J, Zhou Z. Role of intravoxel incoherent motion MRI in preoperative evaluation of DNA mismatch repair status in rectal cancers. Clin Radiol 2019;74:814.e21-8.
41. Li JR, Qi FY, Li L. Correlation between expression of matrix metalloproteinase-2 and angiogenesis in esophageal carcinoma. Zhonghua Zhong Liu Za Zhi 2005;27:96-8.
42. Li-Ou Z, Hong-Zan S, Xiao-Xi B, Zhong-Wei C, Zai-Ming L, Jun X, Qi-Yong G. Correlation between tumor glucose metabolism and multiparametric functional MRI (IVIM and R2*) metrics in cervical carcinoma: Evidence from integrated 18 F-FDG PET/MR. J Magn Reson Imaging 2019;49:1704-12.
43. Gao P, Liu Y, Shi C, Liu Y, Luo L. Performing IVIM-DWI using the multifunctional nanosystem for the evaluation of the antitumor microcirculation changes. MAGMA 2020;33:517-26.
44. Orton MR, Messiou C, Collins D, Morgan VA, Tessier J, Young H, deSouza N, Leach MO. Diffusion-weighted MR imaging of metastatic abdominal and pelvic tumours is sensitive to early changes induced by a VEGF inhibitor using alternative diffusion attenuation models. Eur Radiol 2016;26:1412-9.
45. Koh DM, Collins DJ, Orton MR. Intravoxel incoherent motion in body diffusion-weighted MRI: reality and challenges. AJR Am J Roentgenol 2011;196:1351-61.
46. Yan C, Pan X, Chen G, Ge W, Liu S, Li M, Nie L, He J, Zhou Z. A pilot study on correlations between preoperative intravoxel incoherent motion MR imaging and postoperative histopathological features of rectal cancers. Transl Cancer Res 2017;6:1050-60.
47. Song Q, Guo Y, Yao X, Rao S, Qian C, Ye D, Zeng M. Comparative study of evaluating the microcirculatory function status of primary small HCC between the CE (DCE-MRI) and Non-CE (IVIM-DWI) MR Perfusion Imaging. Abdom Radiol (NY) 2021;46:2575-83.
48. Meyer HJ, Leifels L, Hamerla G, Höhn AK, Surov A. ADC-histogram analysis in head and neck squamous cell carcinoma. Associations with different histopathological features including expression of EGFR, VEGF, HIF-1α, Her 2 and p53. A preliminary study. Magn Reson Imaging 2018;54:214-7.
49. Ma T, Yang S, Jing H, Cong L, Cao Z, Liu Z, Huang Z. Apparent diffusion coefficients in prostate cancer: correlation with molecular markers Ki-67, HIF-1α and VEGF. NMR Biomed 2018.
50. Huang Z, Meng X, Xiu J, Xu X, Bi L, Zhang J, Han X, Liu Q. MR imaging in hepatocellular carcinoma: correlations between MRI features and molecular marker VEGF. Med Oncol 2014;31:313.
51. Li JL, Ye WT, Liu ZY, Yan LF, Luo W, Cao XM, Liang C. Comparison of microvascular perfusion evaluation among IVIM-DWI, CT perfusion imaging and histological microvessel density in rabbit liver VX2 tumors. Magn Reson Imaging 2018;46:64-9.
52. Lindgren A, Anttila M, Rautiainen S, Arponen O, Kivelä A, Mäkinen P, Härmä K, Hämäläinen K, Kosma VM, Ylä-Herttuala S, Vanninen R, Sallinen H. Primary and metastatic ovarian cancer: Characterization by 3.0T diffusion-weighted MRI. Eur Radiol 2017;27:4002-12.
53. Meyer HJ, Gundermann P, Höhn AK, Hamerla G, Surov A. Associations between whole tumor histogram analysis parameters derived from ADC maps and expression of EGFR, VEGF, Hif 1-alpha, Her-2 and Histone 3 in uterine cervical cancer. Magn Reson Imaging 2019;57:68-74.
54. Meyer HJ, Höhn A, Surov A. Histogram analysis of ADC in rectal cancer: associations with different histopathological findings including expression of EGFR, Hif1-alpha, VEGF, p53, PD1, and KI 67. A preliminary study. Oncotarget 2018;9:18510-7.
55. Liu Y, Ye Z, Sun H, Bai R. Grading of uterine cervical cancer by using the ADC difference value and its correlation with microvascular density and vascular endothelial growth factor. Eur Radiol 2013;23:757-65.
56. Min XL, Yang L, Zhang XM, Zhou Y, Miao ND, Ren YJ, Xu H, Liu K, Peng J, Yang K. Changes of tryptase in patients with hepatocellular carcinoma after transarterial chemoembolization. Transl Cancer Res 2017;6:1061-7.
57. Xu PJ, Yan FH, Wang JH, Shan Y, Ji Y, Chen CZ. Contribution of diffusion-weighted magnetic resonance imaging in the characterization of hepatocellular carcinomas and dysplastic nodules in cirrhotic liver. J Comput Assist Tomogr 2010;34:506-12.
58. Peng J, Yang C, Zheng J, Wang R, Zhou Y, Wang W, Yang L, Zhang X, Miao N, Ren Y, Xu H, Min X. Intravoxel Incoherent Motion Diffusion Weighted Imaging for the Therapeutic Response of Transarterial Chemoembolization for Hepatocellular Carcinoma. Journal of Cancer Therapy 2019;10:591-601.
59. Wang YXJ, Huang H, Zheng CJ, Xiao BH, Chevallier O, Wang W. Diffusion-weighted MRI of the liver: challenges and some solutions for the quantification of apparent diffusion coefficient and intravoxel incoherent motion. Am J Nucl Med Mol Imaging 2021;11:107-42.

60. Wáng YXJ. Mutual constraining of slow component and fast component measures: some observations in liver IVIM imaging. Quant Imaging Med Surg 2021;11:2879-87.
61. Wáng YXJ. Observed paradoxical perfusion fraction elevation in steatotic liver: An example of intravoxel incoherent motion modeling of the perfusion component constrained by the diffusion component. NMR Biomed 2021;34:e4488.
62. Xiao BH, Huang H, Wang LF, Qiu SW, Guo SW, Wáng YXJ. Diffusion MRI Derived per Area Vessel Density as a Surrogate Biomarker for Detecting Viral Hepatitis B-Induced Liver Fibrosis: A Proof-of-Concept Study. SLAS Technol 2020;25:474-83.

Cite this article as: Yang C, Wei XQ, Zheng J, Tao YY, Gong XQ, Li L, Li ZM, Yang L, Mao Q, Zhou MT, Zhang XM. A correlative study between IVIM-DWI parameters and VEGF and MMPs expression in hepatocellular carcinoma. Quant Imaging Med Surg 2023;13(3):1887-1898. doi: 10.21037/qims-22-271

